

Effect of Reaction Temperature on Structural, Magnetic and Dielectric Properties of Bismuth Iron Oxide Nanoparticles

*Saira Riaz¹⁾, Farzana Majid²⁾ and Shahzad Naseem¹⁾

*Centre of Excellence in Solid State Physics, University of the Punjab, Lahore 54590,
Pakistan*

**) saira.cssp@pu.edu.pk*

ABSTRACT

During the past few years, multiferroic materials i.e. materials exhibiting ferroelectricity and ferromagnetism have acquired worldwide attraction due to its wide range of applications in devices as small as sensors to devices as large as transformers. Among various multiferroic materials, bismuth iron oxide is a promising candidate. However, there are some drawbacks associated with phase pure BiFeO₃ including volatility of Bi₂O₃, large leakage current and antiferromagnetic/ weak ferromagnetic behavior. In this work bismuth iron oxide nanoparticles (NPs) are synthesized using sol-gel technique. NPs are calcined at 100°C, 200°C and 300°C. Bismuth iron oxide NPs are characterized using x-ray diffractometer, vibrating sample magnetometer and impedance analyzer. NPs show amorphous behavior under as-prepared conditions. Dielectric constant increases from 49 to 74 (at frequency = 1MHz) and tangent loss decreases from 0.2 to 0.012 with increase in calcination temperature from 100-300°C. Ferromagnetic behavior instead of antiferromagnetic nature of bulk bismuth iron oxide arises due to suppression of helical spin structure. The suppression of spin structure leads to ferromagnetic behavior with saturation magnetization of 7.125×10^{-4} emu, 1.28×10^{-3} emu and 1.59×10^{-3} emu at 100°C, 200°C and 300°C.

1. INTRODUCTION

During the past few years, ferroelectric as well as ferromagnetic materials both have acquired worldwide attraction due to its wide range of applications in devices as small as sensors to devices as large as transformers (Arora 2014, Jian 2013). The basic requirement of ferromagnetism is that there must be localized electrons present in the transition metal ion whereas, ferroelectric requirement is an empty shell of electrons. However, there are very few materials that execute both the requirements of ferroelectricity and ferromagnetism (Arora 2014). Among the commonly studied multiferroic materials (exhibiting simultaneous ferroelectric and ferromagnetic

¹⁾ Professor

²⁾ Graduate Student

properties) bismuth iron oxide (BiFeO_3) is the most promising candidate as it has got the highest antiferromagnetic Neel temperature and highest ferroelectric Curie temperature as compared to all other multiferroic materials (Shah 2014 a), Chang 2013).

Bismuth iron oxide (BFO) crystallizes in rhombohedrally distorted perovskite structure at room temperature. It undergoes structural transition to orthorhombic phase near 1098K and to pseudo cubic phase at 1204K. It is an antiferromagnetic with Neel temperature of 647K. Ferromagnetic character in BiFeO_3 arises because of asymmetry in spin that occurs at Fe site. Ferroelectric properties require asymmetry in charge that is present at Bi site (Mocherla 2014, Tripathy 2013, Yan 2014).

However, there are few problems related to BiFeO_3 the most important of which is caused by high volatility of bismuth thus leading to the formation of bismuth deficient $\text{Bi}_2\text{Fe}_4\text{O}_9$ mullite phase along with BiFeO_3 . This can be avoided by using excess of bismuth but excess of bismuth can give rise to bismuth rich $\text{Bi}_{25}\text{FeO}_{40}$ sillenite phase. Another solution to this problem is the use of low temperature synthesis and annealing conditions but in literature the annealing temperature for BFO is reported within the range of 500-600°C Verma 2011, Laughlin 2013, Mocherla 2014, Zhao 2013). So, the control of synthesis and deposition conditions is extremely crucial to get single phase BiFeO_3 (Mazumder 2006, Yan 2014)

For overcoming the difficulties associated with phase pure BFO, we here report the synthesis and characterization of bismuth iron oxide nanoparticles using sol-gel method. The particles are calcined at 100-300°C to observed changes in structural, dielectric and magnetic properties.

2. EXPERIMENTAL DETAILS

For synthesis of bismuth iron oxide nanoparticles, bismuth nitrate and iron nitrate were used as precursors. Iron nitrate and bismuth nitrate were separately dissolved in ethylene glycol. Ethylene glycol, being a linearly structured molecule, helped in compensating for difference in hydrolysis rate of bismuth and iron. The two solutions were mixed together and heated on hot plate at 60°C for several hours. The details of sol-gel synthesis are reported earlier (Shah 2014 (a,b)) The sol was then heat treated at 80°C to obtain BFO nanoparticles (NPs). The NPs were then calcined at 100°C, 200°C and 300°

The NPs were characterized under as prepared conditions. Structural characterizations were carried out using Bruker D8 Advance X-ray Diffractometer. For magnetic measurements Lakeshore's vibrating sample magnetometer was used. Dielectric properties of BFO NPs were carried out in parallel plate configuration using 6500B precision impedance analyzer.

3. RESULTS AND DISCUSSION

Fig. 1 shows XRD pattern of bismuth iron oxide nanoparticles prepared using sol-gel method under as-prepared conditions. The particles show amorphous behavior as can be seen in Fig. 1. The NPs were then calcined at 100-300°C. Transformation from

amorphous to crystalline state was observed with calcination. However, the detailed structural analysis is to be reported elsewhere.

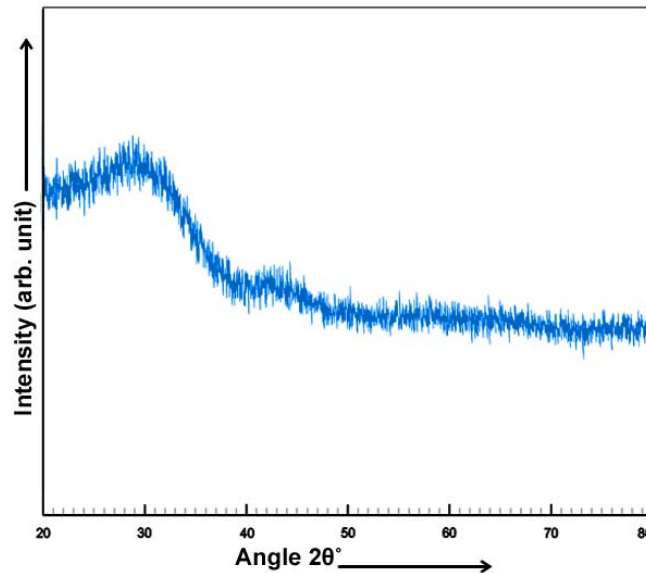


Fig. 1 XRD pattern of bismuth iron oxide nanoparticles prepared using sol-gel method

For studying the dielectric properties of bismuth iron oxide impedance analyzer was used in parallel plate configuration. The parallel capacitance and parallel resistance were measured and then using Eq. 1 and Eq. 2 the dielectric constant ϵ and dielectric loss (tangent loss $\tan \delta$) were calculated.

$$\epsilon = \frac{C \times d}{\epsilon_0 \times A} \quad (1)$$

$$\tan \delta = \frac{1}{2\pi\epsilon\epsilon_0\rho} \quad (2)$$

Where, C is the capacitance, d is the thickness of the specimen, A the area of the device, ϵ_0 is the permittivity of free space and ρ is the resistivity of NPs. NPs show dispersion in low frequency region i.e. dielectric constant and tangent loss decreases as the frequency increases and becomes constant in high frequency region. The dispersion arises as the charge carriers require some time to get align in the direction of externally applied field. At high frequency, the field reversal is so high that the charge carriers have barely moved before field switches again (Arora 2014). The dielectric dispersion curve is explained on the basis of Koop's theory based on Maxwell-Wanger model according to which grain boundaries are found to be more effective in low frequency region while grains are more effective in high frequency region (Verma 2011). It is well known that dielectric properties of thin films are affected by both intrinsic and extrinsic properties. Among the intrinsic parameters film orientation, grain boundaries and dielectric response of single domain is extremely important. Decrease in grain size can lead to increase in internal stresses to inhibit the formation of 180° domain thus causing a decrease in dielectric constant of some multiferroic thin films (Tang 2012).

Dielectric constant of BFO NPs calcined at 100°C, 200°C and 300°C is found to be 49, 71 and 74 ($f = 1\text{MHz}$) with tangent loss of 0.2, 0.0355 and 0.012 respectively. Dielectric constant increases and tangent loss decreases as the calcination temperature is increased from 100°C to 300°C.

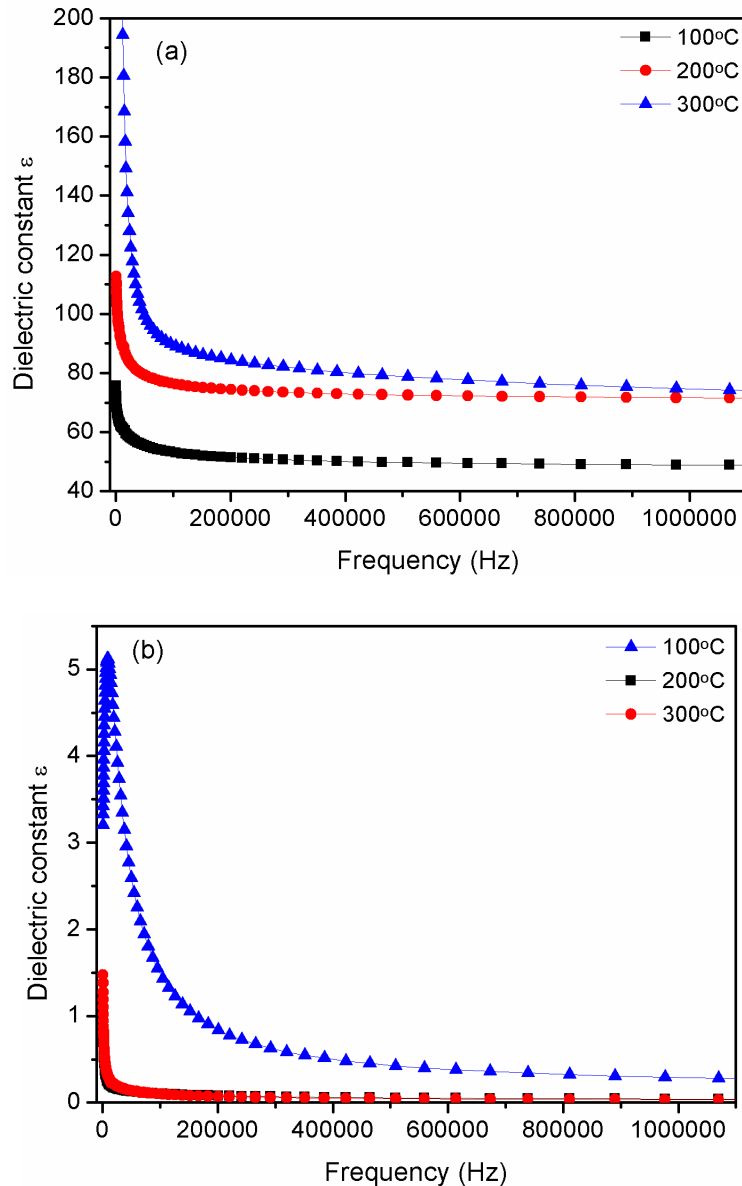


Fig. 2 (a) Dielectric constant (b) tangent loss as a function of frequency

Fig. 3 show M-H curves for bismuth iron oxide NPs prepared using sol-gel method. The NPs show ferromagnetic behavior as opposed to antiferromagnetic nature of bulk bismuth iron oxide. In bulk, bismuth iron oxide shows G-type antiferromagnetic behavior having the magnetic spins that are perpendicular to $[111]_{pc}$ axis located in (111) plane. Within the same plane, ferromagnetic coupling occur between the adjacent spins while with the spins in adjacent planes the coupling is antiferromagnetic. However the spins are not actually perfectly antiparallel. Because of Dzyaloshinskii-Moriya

interaction (anisotropic exchange interaction) canting of spin arrangement occurs. This canting of spiral spin arrangement induces ferromagnetic behavior in BFO that is otherwise antiferromagnetic in nature.

The enhanced magnetic properties in our bismuth iron oxide NPs can be due to: 1) presence of oxygen vacancies (Riaz 2011), 2) canted spin assembly and/or 3) because of suppression of helical spin order. Bismuth iron oxide has a cycloid spin of 620\AA which when suppressed give rise to uncompensated spins. In addition, due to presence of oxygen vacancies in bismuth iron oxide structure Fe^{2+} cations are introduced in Fe^{3+} - O^{2-} - Fe^{2+} order thus, enhancing the magnetic properties (Jian 2013, Shah 2014(b)).

Saturation magnetization of bismuth iron oxide NPs increases as the calcination temperature is increased. Saturation magnetization for NPs calcined at 100°C , 200°C and 300°C is 7.125×10^{-4} emu, 1.28×10^{-3} emu and 1.59×10^{-3} emu respectively.

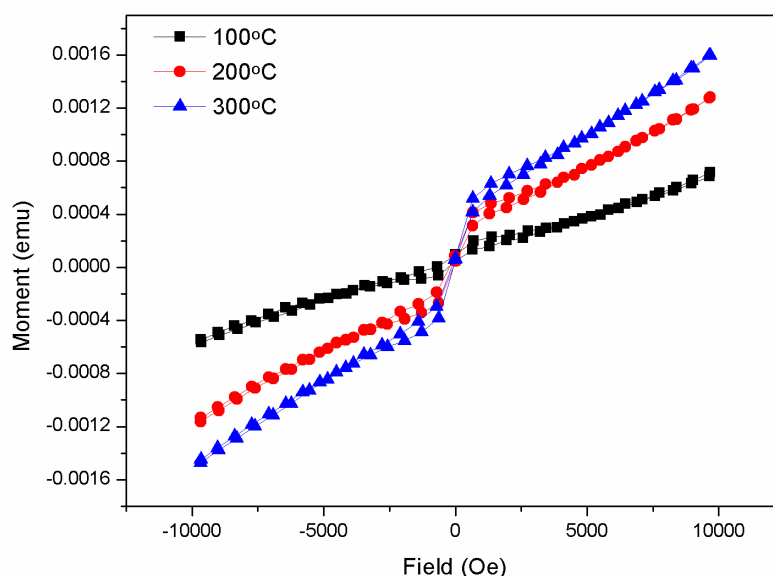


Fig. 3 M-H curves for bismuth iron oxide nanoparticles

4. CONCLUSIONS

Bismuth iron oxide nanoparticles were prepared using sol-gel method. The nanoparticles are calcined at 100°C , 200°C and 300°C . As-prepared nanoparticles show amorphous behavior. With increase in calcination temperature from 100 - 300°C , dielectric constant increases from 49 to 74 ($f = 1\text{MHz}$) and tangent loss decreases from 0.2 to 0.012 with increase in calcination temperature. Bismuth iron oxide nanoparticles show ferromagnetic behavior with saturation magnetization of 1.59×10^{-3} emu. Ferromagnetic behavior in otherwise antiferromagnetic bismuth iron oxide arises as the helical spin structure is suppressed thus, converting to linear spin structure.

REFERENCES

- Arora, M., Chauhan, S., Sati, P.C. and Kumar, M. (2014), "Effect of non-magnetic ions substitution on structural, magnetic and optical properties of BiFeO₃ nanoparticles," *J. Supercond. Nov. Magn.*, DOI 10.1007/s10948-014-2521-4
- Chang, H.W., Yuan, F.Y., Tien, S.H., Li, P.Y., Wang, C.R., Tu, C.S. and Jen, S.U. (2013), "High quality multiferroic BiFeO₃ films prepared by pulsed laser deposition on glass substrates at reduced temperatures," *J. Appl. Phys.*, **113**, 17D917
- Jian, S.R., Chang, H.W., Tseng, Y.C., Chen, P.H. and Juang, J.Y. (2013), "Structural and nanomechanical properties of BiFeO₃ thin films deposited by radio frequency magnetron sputtering," *Nanoscale Res. Lett.*, **8**, 297
- Laughlin, R.P., Currie, D.A., Guerro, R.C., Dedigama, A., Priyantha, W., Droopad, R., Theodoropoulou, N., Gao, P. and Pan, X. (2013), "Magnetic and structural properties of BiFeO₃ thin films grown epitaxially on SrTiO₃/Si substrates," *J. Appl. Phys.*, **113**, 17D919
- Mazumder, R., Ghosh, S., Mondal, P., Bhattacharya, D., S. Dasgupta, S., Das, N. and Sen, A. (2006), "Particle size dependence of magnetization and phase transition near T_N in multiferroic BiFeO₃," *J. Appl. Phys.*, **100**, 033908
- Mocherla, P.S.V., Karthik, C., Ubic, R., Rao, M.S.R. and C. Sudakar, C. (2014), "Tunable bandgap in BiFeO₃ nanoparticles: The role of microstrain and oxygen defects," *Appl. Phys. Lett.*, **103**, 022910.
- Riaz, S. and Naseem, S., Xu, Y.B. (2011), "Room temperature ferromagnetism in sol-gel deposited un-doped ZnO films," *J. Sol-Gel Sci. Technol.*, **59**, 584–590
- Shah, S.M.H., Akbar, A., Riaz, S., Atiq, S. and Naseem, S. (2014(a)), "Magnetic, structural and dielectric properties of Bi_{1-x}K_xFeO₃ thin films using sol-gel" *IEEE. Trans. Magn.*, DOI: 10.1109/TMAG.2014.2310691
- Shah, S.M.H., Riaz, S., Akbar, A., Atiq, S. and Naseem, S. (2014(b)), "Effect of solvents on the ferromagnetic behavior of un-doped BiFeO₃ prepared by sol-gel," *IEEE. Trans. Magn.*, DOI: 10.1109/TMAG.2014.2309720
- Tang, X., Dai, J., Zhu, X., Lin, J., Chang, Q., Wu, D., Song, W. and Sun, Y. (2012), "Thickness-dependent dielectric, ferroelectric, and magnetodielectric properties of BiFeO₃ thin films derived by Chemical Solution Deposition." *J. Am. Ceram. Soc.*, **95**(2), 538–544.
- Tripathy, S.N., Mishra, B.G., Shirolkar, M.M., Sen, S., Das, S.R., Janes, D.B. and Pradhan, D.K. (2013), "Structural, microstructural and magneto-electric properties of single-phase BiFeO₃ nanoceramics prepared by auto-combustion method," *Mater. Chem. Phys.*, **141**, 423-431
- Verma, K.C., Ram, M., Singh, J. and Kotnala, R.K. (2011), "Impedance spectroscopy and dielectric properties of Ce and La substituted Pb_{0.7}Sr_{0.3}(Fe_{0.012}Ti_{0.988})O₃ nanoparticles." *J. Alloys Compd.*, **509**, 4967–4971.
- Yan, D., Sun, C., Jian, J., Sun, Y., Wu, R. and Li, J. (2014), "Structure and phase transition of BiFeO₃ particles prepared by hydrothermal method and the verification of crystallization– dissolution–crystallization mechanism," *J. Mater. Sci.: Mater. Electron.*, **25**, 928–935.
- Zhao, J., Liu, S., Zhang, W., Liu, Z. and Liu, Z. (2013), "Structural and magnetic properties of Er-doped BiFeO₃ nanoparticles," *J. Nanopart. Res.*, **15**, 1969